

Critical endpoint in the Polyakov-loop extended NJL model

Kouji Kashiwa,^{1,*} Hiroaki Kouno,^{2,†} Masayuki Matsuzaki,^{3,‡} and Masanobu Yahiro^{1,§}

¹*Department of Physics, Graduate School of Sciences,*

Kyushu University, Fukuoka 812-8581, Japan

²*Department of Physics, Saga University, Saga 840-8502, Japan*

³*Department of Physics, Fukuoka University of Education,*

Munakata, Fukuoka 811-4192, Japan

(Dated: February 2, 2008)

Abstract

The critical endpoint (CEP) and the phase structure are studied in the Polyakov-loop extended Nambu–Jona-Lasinio model in which the scalar type eight-quark (σ^4) interaction and the vector type four-quark interaction are newly added. The σ^4 interaction largely shifts the CEP toward higher temperature and lower chemical potential, while the vector type interaction does oppositely. At zero chemical potential, the σ^4 interaction moves the pseudo-critical temperature of the chiral phase transition to the vicinity of that of the deconfinement phase transition.

PACS numbers: 11.30.Rd, 12.40.-y

*kashiwa2scp@mbox.nc.kyushu-u.ac.jp

†kounoh@cc.saga-u.ac.jp

‡matsuza@fukuoka-edu.ac.jp

§yahiro2scp@mbox.nc.kyushu-u.ac.jp

The position of the critical endpoint (CEP) in the phase diagram is one of the most interesting subjects in hot and dense Quantum Chromodynamics (QCD). With the aid of the progress in computer power, lattice QCD simulations have become feasible for thermal systems at zero chemical potential (μ) [1]. For finite chemical potential, however, lattice QCD has the well-known sign problem, so that only a few works were made to determine the position of the CEP [2, 3].

As an approach complementary to first-principle lattice simulations, one can consider several effective models. One of them is the Nambu–Jona-Lasinio (NJL) model [4]. In the original NJL model that includes scalar and pseudo-scalar type four-quark interactions, it was found that there exists a CEP in the phase diagram [5, 6]. However, the CEP is located at a lower temperature (T) and a higher μ compared with the one predicted by a lattice QCD simulation [2] and by the QCD-like theory [7, 8]. Moreover, recent empirical analysis [9] of η/s , the ratio of shear viscosity to entropy density, suggest there is a CEP at $T_e \sim 165$ MeV and $\mu_e \sim 50 - 60$ MeV that is much higher T and lower μ than the NJL model predictions.

Kashiwa et al. [10] showed that in the NJL model the scalar type eight-quark (σ^4) interaction newly added shifts the CEP toward higher T and lower μ . However, the location is still far from predictions of lattice QCD, the QCD-like theory and the empirical analyses.

It is also known in the chiral hadron model [11, 12] that a CEP appears at T much higher than the prediction of the NJL model. This implies that the deconfinement phase transition plays an important role in determining the position of the CEP. Although the NJL model is a useful method for understanding the chiral symmetry breaking, this model does not possess a confinement mechanism. As a reliable model that can treat both the chiral and the deconfinement phase transitions, we can consider the Polyakov-loop extended NJL (PNJL) model [13, 14, 15, 16, 17, 18, 19, 20, 21, 22]. In the PNJL model the confinement/deconfinement phase transition is described by the Polyakov loop. Effects of the Polyakov loop make the CEP move to higher T and lower μ than the NJL model predicts [19]. The position of the CEP is still far from the predictions of lattice QCD and the empirical analyses.

Meanwhile, it was recently reported that the vector type interaction [10, 23, 24, 25] is necessary to realize the heavy neutron star [26]. This may indicate that the vector type interaction is necessary in the finite μ region of the phase diagram.

In this letter, we study effects of the σ^4 and the vector type interactions on the position

of the CEP and the interplay between the chiral and the deconfinement phase transitions, by using the PNJL model with these interactions.

The model we consider here is the following two-flavor PNJL model with the vector type interaction [10, 23, 24, 25] and the σ^4 interaction [10, 27, 28, 29, 30]

$$\mathcal{L} = \bar{q}(i\gamma_\mu D^\mu - m_0)q + \mathcal{L}_{\text{int}} - \mathcal{U}(\Phi[A], \bar{\Phi}[A], T), \quad (1)$$

where q denotes the two-flavor quark field, m_0 the current quark mass and $D^\mu = \partial^\mu - iA^\mu$ the covariant derivative. The field A^μ is defined as $A^\mu = \delta_{\mu 0} g A_a^\mu \frac{\lambda_a}{2}$ with the gauge field A_a^μ , the Gell-Mann matrix λ_a and the gauge coupling g . The interaction of the NJL sector, \mathcal{L}_{int} , is

$$\mathcal{L}_{\text{int}} = G_s[(\bar{q}q)^2 + (\bar{q}i\gamma_5\vec{\tau}q)^2] + G_{s8}[(\bar{q}q)^2 + (\bar{q}i\gamma_5\vec{\tau}q)^2]^2 - G_v(\bar{q}\gamma^\mu q)^2, \quad (2)$$

where $\vec{\tau}$ stands for the isospin matrix, and G_s , G_v and G_{s8} denote coupling constants of the scalar type four-quark, the vector type four-quark and the σ^4 interactions, respectively. The Polyakov potential \mathcal{U} , defined in Eq. (15), is a function of the Polyakov loop Φ and its conjugate $\bar{\Phi}$,

$$\Phi = \frac{1}{N_c}(\text{Tr}L), \quad \bar{\Phi} = \frac{1}{N_c}(\text{Tr}L^\dagger), \quad (3)$$

with

$$L(\mathbf{x}) = \mathcal{P} \exp \left[i \int_0^\beta d\tau A_4(\mathbf{x}, \tau) \right], \quad (4)$$

where \mathcal{P} is the path ordering and $A_4 = iA_0$. In the chiral limit ($m_0 = 0$), the Lagrangian density has exact $SU(2)_L \times SU(2)_R \times U(1)_v \times SU(3)_c$ symmetry.

The temporal component of the gauge field is diagonal in the flavor space, because the color and the flavor spaces are completely separated out in the present case. In the Polyakov gauge, the Polyakov loop matrix L can be written in a diagonal form in the color space [14]:

$$\frac{1}{N_c}(\text{Tr}L) = \frac{1}{N_c}(\text{Tr} e^{i\beta(\phi_3\lambda_3 + \phi_8\lambda_8)}), \quad (5)$$

$$= \frac{1}{N_c} \left(\text{Tr} \text{diag}(e^{i\beta\phi_a}, e^{i\beta\phi_b}, e^{i\beta\phi_c}) \right), \quad (6)$$

where $\phi_a = \phi_3 + \phi_8/\sqrt{3}$, $\phi_b = -\phi_3 + \phi_8/\sqrt{3}$ and $\phi_c = -(\phi_a + \phi_b) = -2\phi_8/\sqrt{3}$. The Polyakov loop is an exact order parameter of the spontaneous $\mathbb{Z}(N_c)$ symmetry breaking

in the pure gauge theory. Although $\mathbb{Z}(N_c)$ is not an exact symmetry in the system with dynamical quarks, it still seems to be a good indicator of the deconfinement phase transition. Therefore, we use Φ to define the deconfinement phase transition.

Under the mean field approximation (MFA), the Lagrangian density becomes

$$\mathcal{L}_{\text{MFA}} = \bar{q}(i\gamma_\mu D^\mu - (m_0 + \Sigma_s) + \Sigma_v \gamma^0)q - U(\sigma, \rho_v) - \mathcal{U}(\Phi, \bar{\Phi}, T), \quad (7)$$

where

$$\sigma = \langle \bar{q}q \rangle, \quad \rho_v(T, \mu, \sigma, \Phi, \bar{\Phi}) = \langle \bar{q}\gamma_0 q \rangle, \quad (8)$$

$$\Sigma_s = -(2G_s\sigma + 4G_{s8}\sigma^3), \quad \Sigma_v = -2G_v\rho_v, \quad (9)$$

$$U = G_s\sigma^2 + 3G_{s8}\sigma^4 - G_v\rho_v^2. \quad (10)$$

In the $1/N_c$ expansion, the eight-quark interaction after the MFA, $\bar{q}\Gamma q\langle\bar{q}\Gamma'q\rangle^3$ is of order N_c^0 and accordingly the same order as the four-quark interaction after the MFA, $\bar{q}\Gamma q\langle\bar{q}\Gamma'q\rangle$, where Γ and Γ' are vertex matrices. Therefore, we can not ignore higher multi-quark interactions in general. As a starting point, we take into account the scalar type eight-quark (σ^4) interaction that is known to affect the position of the CEP [10]. Using the usual techniques [31, 32], one can obtain the thermodynamical potential

$$\Omega = -T \ln Z \quad (11)$$

$$\begin{aligned} &= -2N_f V \int \frac{d^3\mathbf{p}}{(2\pi)^3} \left[3E(\mathbf{p}) + \frac{1}{\beta} \left\{ \text{Tr}_c \ln(1 + L e^{-\beta E^-(\mathbf{p})}) \right. \right. \\ &\quad \left. \left. + \text{Tr}_c \ln(1 + L^\dagger e^{-\beta E^+(\mathbf{p})}) \right\} \right] + \left\{ U(\sigma, \omega) + \mathcal{U}(\bar{\Phi}, \Phi, T) \right\} V, \end{aligned} \quad (12)$$

where $E(\mathbf{p}) = \sqrt{\mathbf{p}^2 + M^2}$, $E^\pm = E(\mathbf{p}) \pm \tilde{\mu}$, $M = m_0 + \Sigma_s$ and $\tilde{\mu} = \mu + \Sigma_v$. After some algebra, the thermodynamical potential Ω becomes [17]

$$\begin{aligned} \Omega &= -2N_f V \int \frac{d^3\mathbf{p}}{(2\pi)^3} \left[3E(\mathbf{p}) \right. \\ &\quad + \frac{1}{\beta} \ln [1 + 3(\Phi + \bar{\Phi} e^{-\beta E^-(\mathbf{p})}) e^{-\beta E^-(\mathbf{p})} + e^{-3\beta E^-(\mathbf{p})}] \\ &\quad + \frac{1}{\beta} \ln [1 + 3(\bar{\Phi} + \Phi e^{-\beta E^+(\mathbf{p})}) e^{-\beta E^+(\mathbf{p})} + e^{-3\beta E^+(\mathbf{p})}] \\ &\quad \left. + (U + \mathcal{U})V \right] \end{aligned} \quad (13)$$

In the $T = 0$ limit, the PNJL model is reduced to the NJL model, since the Polyakov

loop is included only in \mathcal{U} that has no σ dependence, as shown in

$$\begin{aligned} \Omega = & -6N_f V \int \frac{d^3\mathbf{p}}{(2\pi)^3} \left[E(\mathbf{p}) - \theta(-E^-(\mathbf{p}))E^-(\mathbf{p}) \right] \\ & + \left[U(\sigma, \rho_v(T \rightarrow 0, \mu, \sigma)) + \mathcal{U}(T \rightarrow 0, \Phi, \bar{\Phi}) \right] V. \end{aligned} \quad (14)$$

We use \mathcal{U} of Ref. [17] that is fitted to a lattice QCD simulation in the pure gauge theory at finite T [33, 34]:

$$\frac{\mathcal{U}}{T^4} = -\frac{b_2(T)}{2}\bar{\Phi}\Phi - \frac{b_3}{6}(\bar{\Phi}^3 + \Phi^3) + \frac{b_4}{4}(\bar{\Phi}\Phi)^2, \quad (15)$$

$$b_2(T) = a_0 + a_1\left(\frac{T_0}{T}\right) + a_2\left(\frac{T_0}{T}\right)^2 + a_3\left(\frac{T_0}{T}\right)^3, \quad (16)$$

where parameters are summarized in Table I.

The Polyakov potential yields a deconfinement phase transition at $T = T_0$ in the pure gauge theory. Hence, T_0 is taken to be 270 MeV predicted by the pure gauge lattice QCD calculation.

a_0	a_1	a_2	a_3	b_3	b_4
6.75	-1.95	2.625	-7.44	0.75	7.5

TABLE I: Summary of the parameter set in the Polyakov sector used in Ref. [17]. All parameters are dimensionless.

Since the NJL model is nonrenormalizable, it is needed to introduce a cutoff in the momentum integration. In this study, we use the three-dimensional momentum cutoff

$$\int \frac{d^3\mathbf{p}}{(2\pi)^3} \rightarrow \frac{1}{2\pi^2} \int_0^\Lambda p^2 dp. \quad (17)$$

Hence, the present model has five parameters m_0 , Λ , G_s , G_{s8} , and G_v in the NJL sector. We simply assume $m_0 = 5.5$ MeV. In the case without the σ^4 interaction, we use $\Lambda = 0.6315$ GeV and $G_s = 5.498$ GeV⁻², which reproduce the empirical values of the pion decay constant and the pion mass, $f_\pi = 93.3$ MeV and $M_\pi = 138$ MeV. In the case with the σ^4 interaction, we take $\Lambda = 0.6315$ GeV, $G_s = 5.002$ (5.276) GeV⁻² and $G_{s8}\sigma_0^2 = 0.2476$ GeV⁻² (0.1109 GeV⁻²), which reproduce the pion decay constant $f_\pi = 93.3$ MeV, the pion mass $M_\pi = 138$ MeV and the sigma meson mass $M_\sigma = 600$ MeV (650 MeV) [10]. It should be noted that larger G_{s8} yields smaller M_σ .

For the vector coupling constant G_v , we take three values, 0, $0.25G_s$ and $0.5G_s$. The case $G_v = 0.5G_s$ is obtained by one gluon exchange calculation in perturbative QCD [35]. The case $G_v = 0.25G_s$ is obtained by the instanton-anti-instanton molecule model [24].

Table II summarizes the parameter sets we take.

model	G_s	$G_{s8}\sigma_0^2$
Original	5.498	0
Original + σ^4	5.002	0.2476
Original + σ^4 ($M_\sigma = 650$ MeV)	5.276	0.1109

TABLE II: Summary of the parameter sets of the NJL part. The coupling constants are shown in GeV^{-2} . For all cases, we take $\Lambda = 0.6315$ GeV and $\sigma_0 \equiv \sigma(T=0, \mu=0) = -0.03023$ GeV^3 .

Stationary conditions for σ , ρ_v , Φ and $\bar{\Phi}$ become

$$\frac{1}{V} \frac{\partial \Omega}{\partial \sigma} = G_s^* \sigma + 6N_f G_s^* \times \int \frac{d^3 p}{(2\pi)^3} \left\{ \frac{M}{E(\mathbf{p})} \left\{ 1 - \frac{h^{(-)}(\sigma, \Phi, \bar{\Phi}; T, \mu)}{g^{(-)}(\sigma, \Phi, \bar{\Phi}; T, \mu)} - \frac{h^{(+)}(\sigma, \Phi, \bar{\Phi}; T, \mu)}{g^{(+)}(\sigma, \Phi, \bar{\Phi}; T, \mu)} \right\} \right\} = 0, \quad (18)$$

$$\frac{1}{V} \frac{\partial \Omega}{\partial \rho_v} = -2G_v \rho_v + 12N_f G_v \times \int \frac{d^3 p}{(2\pi)^3} \left\{ \frac{h^{(-)}(\sigma, \Phi, \bar{\Phi}; T, \mu)}{g^{(-)}(\sigma, \Phi, \bar{\Phi}; T, \mu)} - \frac{h^{(+)}(\sigma, \Phi, \bar{\Phi}; T, \mu)}{g^{(+)}(\sigma, \Phi, \bar{\Phi}; T, \mu)} \right\} = 0, \quad (19)$$

$$\frac{1}{V} \frac{\partial \Omega}{\partial \Phi} = \frac{T^4}{2} (-b_2(T)\Phi - b_3\bar{\Phi}^2 + b_4\bar{\Phi}\Phi^2) - 6N_f T \int \frac{d^3 p}{(2\pi)^3} \left\{ \frac{e^{-2\beta E^-(\mathbf{p})}}{g^{(-)}(\sigma, \Phi, \bar{\Phi}; T, \mu)} + \frac{e^{-\beta E^+(\mathbf{p})}}{g^{(+)}(\sigma, \Phi, \bar{\Phi}; T, \mu)} \right\} = 0, \quad (20)$$

$$\frac{1}{V} \frac{\partial \Omega}{\partial \bar{\Phi}} = \frac{T^4}{2} (-b_2(T)\bar{\Phi} - b_3\Phi^2 + b_4\bar{\Phi}^2\Phi) - 6N_f T \int \frac{d^3 p}{(2\pi)^3} \left\{ \frac{e^{-\beta E^-(\mathbf{p})}}{g^{(-)}(\sigma, \Phi, \bar{\Phi}; T, \mu)} + \frac{e^{-2\beta E^+(\mathbf{p})}}{g^{(+)}(\sigma, \Phi, \bar{\Phi}; T, \mu)} \right\} = 0, \quad (21)$$

with

$$g^{(-)}(\sigma, \Phi, \bar{\Phi}; T, \mu) = 1 + 3(\Phi + \bar{\Phi}e^{-\beta E^-(\mathbf{p})})e^{-\beta E^-(\mathbf{p})} + e^{-3\beta E^-(\mathbf{p})}, \quad (22)$$

$$g^{(+)}(\sigma, \Phi, \bar{\Phi}; T, \mu) = 1 + 3(\bar{\Phi} + \Phi e^{-\beta E^+(\mathbf{p})})e^{-\beta E^+(\mathbf{p})} + e^{-3\beta E^+(\mathbf{p})}, \quad (23)$$

$$h^{(-)}(\sigma, \Phi, \bar{\Phi}; T, \mu) = \Phi e^{-\beta E^-(\mathbf{p})} + 2\bar{\Phi}e^{-2\beta E^-(\mathbf{p})} + e^{-3\beta E^-(\mathbf{p})}, \quad (24)$$

$$h^{(+)}(\sigma, \Phi, \bar{\Phi}; T, \mu) = \bar{\Phi}e^{-\beta E^+(\mathbf{p})} + 2\Phi e^{-2\beta E^+(\mathbf{p})} + e^{-3\beta E^+(\mathbf{p})}, \quad (25)$$

where the effective coupling G_s^* is defined as $G_s^* = 2G_s + 12G_{s8}\sigma^2$.

Values of σ are directly determined from minima of the real part of the thermodynamical potential, while Φ , $\bar{\Phi}$ and ρ_v are obtained by solving Eqs. (18)-(21).

Following Refs. [14, 21], we define the susceptibilities as

$$\chi = C^{-1}$$

$$= \frac{1}{\det C} \begin{pmatrix} C_{\Phi\Phi}C_{\bar{\Phi}\bar{\Phi}} - C_{\Phi\bar{\Phi}}C_{\bar{\Phi}\Phi} & C_{\sigma\bar{\Phi}}C_{\bar{\Phi}\sigma} - C_{\sigma\Phi}C_{\bar{\Phi}\bar{\Phi}} & C_{\sigma\Phi}C_{\Phi\bar{\Phi}} - C_{\sigma\bar{\Phi}}C_{\Phi\Phi} \\ C_{\Phi\bar{\Phi}}C_{\bar{\Phi}\sigma} - C_{\Phi\sigma}C_{\bar{\Phi}\bar{\Phi}} & C_{\sigma\sigma}C_{\bar{\Phi}\bar{\Phi}} - C_{\sigma\bar{\Phi}}C_{\bar{\Phi}\sigma} & C_{\sigma\bar{\Phi}}C_{\Phi\sigma} - C_{\sigma\sigma}C_{\bar{\Phi}\bar{\Phi}} \\ C_{\Phi\sigma}C_{\bar{\Phi}\Phi} - C_{\Phi\bar{\Phi}}C_{\bar{\Phi}\sigma} & C_{\sigma\sigma}C_{\bar{\Phi}\sigma} - C_{\sigma\sigma}C_{\bar{\Phi}\bar{\Phi}} & C_{\sigma\sigma}C_{\Phi\Phi} - C_{\sigma\Phi}C_{\Phi\sigma} \end{pmatrix}, \quad (26)$$

$$\chi_{ij} = C_{ij}^{-1} \quad (i, j = \sigma, \Phi, \bar{\Phi}), \quad (27)$$

where C is the matrix of dimensionless curvatures

$$C = \begin{pmatrix} \frac{\beta}{4G_s^2\Lambda} \frac{\partial^2 \Omega}{\partial \sigma^2} & -\frac{\beta}{2G_s\Lambda^2} \frac{\partial^2 \Omega}{\partial \sigma \partial \Phi} & -\frac{\beta}{2G_s\Lambda^2} \frac{\partial^2 \Omega}{\partial \sigma \partial \bar{\Phi}} \\ -\frac{\beta}{2G_s\Lambda^2} \frac{\partial^2 \Omega}{\partial \Phi \partial \sigma} & \frac{\beta}{\Lambda^3} \frac{\partial^2 \Omega}{\partial \Phi^2} & \frac{\beta}{\Lambda^3} \frac{\partial^2 \Omega}{\partial \Phi \partial \bar{\Phi}} \\ -\frac{\beta}{2G_s\Lambda^2} \frac{\partial^2 \Omega}{\partial \bar{\Phi} \partial \sigma} & \frac{\beta}{\Lambda^3} \frac{\partial^2 \Omega}{\partial \bar{\Phi} \partial \Phi} & \frac{\beta}{\Lambda^3} \frac{\partial^2 \Omega}{\partial \bar{\Phi}^2} \end{pmatrix}. \quad (28)$$

In this study, the susceptibility is used to determine a pseudo-critical temperature of crossover.

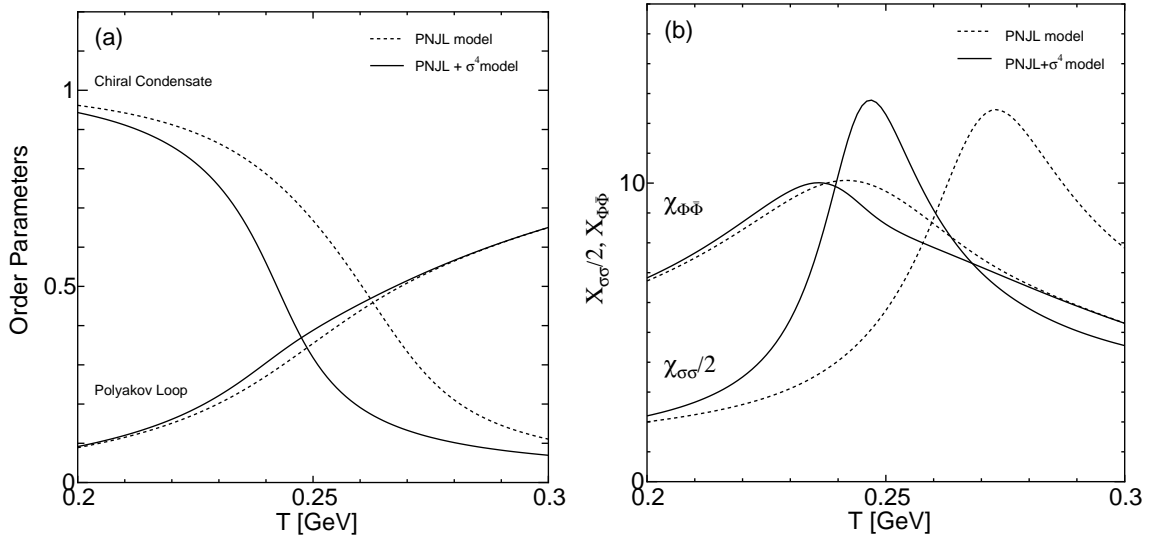


Fig. 1: The left panel graphs the T dependence of the chiral condensate $\langle \bar{q}q \rangle / \langle \bar{q}q \rangle_{T=\mu=0}$ and the Polyakov loop Φ at $\mu = 0$. The right panel graphs the chiral and Polyakov loop susceptibilities.

First we discuss the T dependence of the chiral condensate, the Polyakov loop and their susceptibilities in the case of $\mu = 0$. Figure 1 shows two results of the original PNJL and

the PNJL+ σ^4 models, since the vector type interaction does not contribute to the phase transition when $\mu = 0$. From the left panel, we can see that the σ^4 interaction makes the chiral phase transition sharper and its pseudo-critical temperature lower in the PNJL model as well as in the NJL model [10]. Similar effects are also seen in the three flavor NJL model [29, 30]. Meanwhile, the σ^4 interaction affects the Polyakov loop little. As a result, the pseudo-critical temperature of the chiral phase transition goes down to the vicinity of that of the deconfinement transition.

The pseudo-critical temperatures are calculated also in Refs. [17, 20]. Our regularization scheme is the same as that of Ref. [20] but not as that of Ref. [17], that is, in the present work the momentum cutoff is taken for both the vacuum and T -dependent terms in the square bracket of Eq. (12), while in Ref. [17] the cutoff is made only for the vacuum term. Consequently, our result is consistent with that of Ref. [20], but somewhat deviates from that of Ref. [17].

The pseudo-critical temperatures (T_c) can be clearly defined by the peak of the susceptibilities, as shown in the right panel of Fig.1. In the original PNJL model the pseudo-critical temperatures of the chiral and the deconfinement phase transitions are $T_c = 273$ MeV and 242 MeV, respectively. In the PNJL + σ^4 model, the corresponding values are $T_c = 247$ MeV and 236 MeV. The differences between the chiral and the deconfinement pseudo-critical temperatures are 31 MeV in the original PNJL model and 11 MeV in the PNJL+ σ^4 model. Thus, the σ^4 interaction makes the difference smaller.

Second we discuss the behavior of the chiral condensate and the Polyakov loop near the CEP (T_e, μ_e). Figure 2 shows the T dependence of the chiral condensate, the Polyakov loop and their susceptibilities near the CEP. As clearly seen in the right panel, both the chiral and Polyakov loop susceptibilities diverge at the CEP. This indicates that the two phase transitions are second order at the CEP. Further discussions on the CEP will be made in a forthcoming paper.

Finally we show the phase diagram in Fig. 3. In the region of $T < T_e$ and $\mu > \mu_e$ the chiral and deconfinement transitions are first order and occur at the same time. This can be understood by the generalized Clausius-Clapeyron relation for systems with multiple order parameters, which ensures that their discontinuities appear at the same T and μ when all the transitions are first order [36]. Thus, the deconfinement phase transition seems to be dragged by the chiral phase transition.

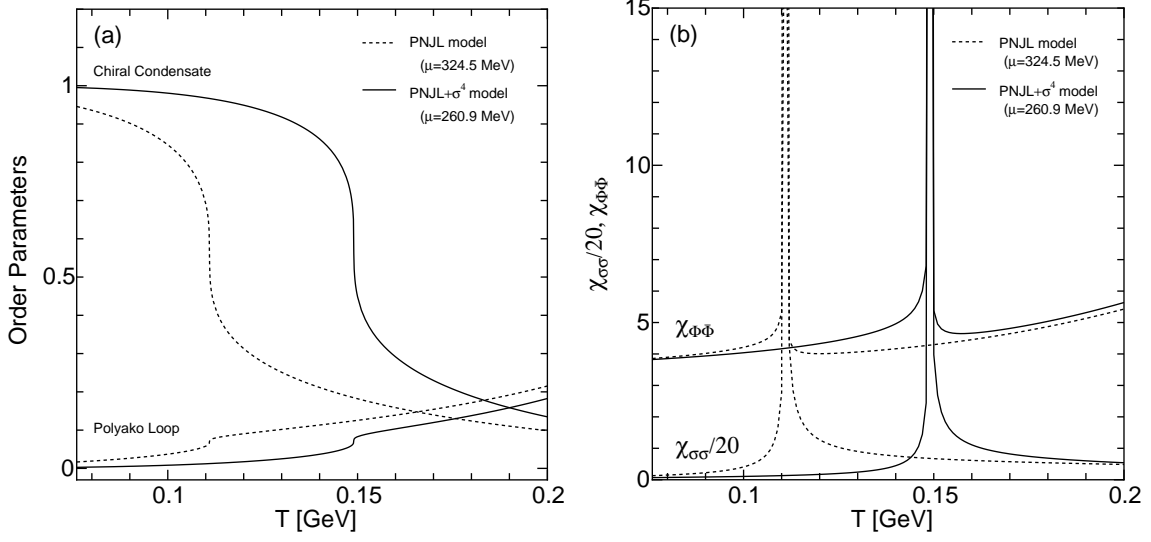


Fig. 2: The left panel graphs the T dependence of the chiral condensate $\langle\bar{q}q\rangle/\langle\bar{q}q\rangle_{T=\mu=0}$ and the Polyakov loop Φ near the CEP. The right panel graphs the chiral and Polyakov loop susceptibilities.

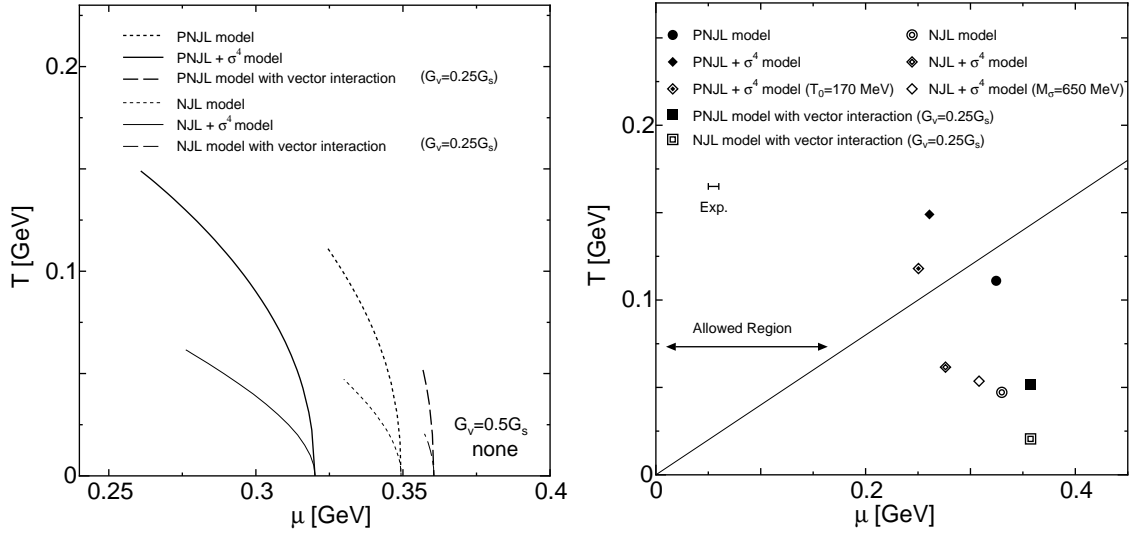


Fig. 3: The left panel graphs the phase diagram on the $T-\mu$ plane. The right panel shows positions of the CEP in several versions of the NJL model and the PNJL model. The allowed region of the μ_e/T_e suggested by a lattice simulation is also indicated. The values of T_e and μ_e in several models are explicitly given in Table III.

It is known [21] that the Polyakov loop susceptibility has a broad bump in the larger T region in addition to a sharp peak in the smaller T region. In Ref. [21], the sharp peak was interpreted as a reflection of the chiral phase transition and the broad bump was then identified with the critical temperature for the deconfinement phase transition. The broad bump does not disappear even if the σ^4 interaction is introduced. However, we simply define the critical temperature with the sharp peak. The critical temperature thus defined for the deconfinement phase transition approaches that for the chiral phase transition as μ increases to μ_e , and both the critical temperatures agree with each other when $\mu \geq \mu_e$. This behavior is consistent with the generalized Clausius-Clapeyron relation among multiple first-order phase transitions [36].

The left panel of Fig. 3 shows phase transition lines of six models. Comparing the original PNJL and the PNJL+ σ^4 models, we see that the σ^4 interaction makes the CEP move toward higher T and lower μ . Meanwhile, comparison between the original PNJL model and the PNJL model with vector interaction shows that the vector type interaction makes the first-order phase transition weak and does the CEP move toward lower T and higher μ , that is, in the direction opposite to the case of the σ^4 interaction. The CEP in the PNJL model is always located at T higher than that in the NJL model, even if either the vector or the σ^4 interaction are added to the models.

The right panel of Fig. 3 shows positions of the CEP in several versions of the NJL and the PNJL models. Results of all models are far from the empirical value, but the result of the PNJL+ σ^4 model is closest. It is suggested in the recent lattice analysis [3] that the possible region where the CEP exists is $\mu_e/T_e \lesssim 2.5$. The allowed region is denoted by the bidirectional arrow in the right panel. Only the PNJL+ σ^4 model satisfies this restriction. So far we took $T_0=270$ MeV, but the pseudo-critical temperature T_c evaluated by adopting this value of T_0 is somewhat higher than the prediction of a lattice QCD calculation [37]. So, we have rescaled T_0 so that the average of the chiral and deconfinement pseudo-critical temperatures can agree with that of the lattice QCD at $\mu = 0$. The rescaled T_0 is 170 MeV. The CEP given by the PNJL+ σ^4 model yields $\mu_e/T_e \sim 1.8$ when $T_0=270$ MeV and 2.1 when $T_0=170$ MeV. Both the results satisfy the restriction $\mu_e/T_e \lesssim 2.5$. Moreover, the latest lattice analysis [3] points out $T_e/T_c \sim 0.8$. The ratio calculated with the PNJL+ σ^4 model is 0.6-0.7 in both cases of $T_0=170$ and 270 MeV and consistent with the prediction of the lattice analysis [3].

In summary, we have investigated effects of the σ^4 and the vector interactions on the position of the CEP and the interplay between the chiral and deconfinement phase transitions. In the case of $\mu = 0$, the σ^4 interaction shifts the pseudo-critical temperature of the chiral transition to the vicinity of that of the deconfinement transition. As for the CEP, the σ^4 interaction shifts it largely toward higher T and lower μ , while the vector type interaction shifts it in the opposite direction. The CEP calculated with the PNJL+ σ^4 model is closest to the empirical one and is in good agreement with the restriction $\mu_e/T_e \lesssim 2.5$ given by the recent lattice analysis. Thus, it is quite interesting to investigate roles of the σ^4 interaction in other thermodynamic quantities such as pressure and quark number density.

Acknowledgments

The authors thank Prof. M. Tachibana for useful discussions. H.K. also thanks Prof. T. Kunihiro, Prof. M. Imachi and Prof. H. Yoneyama for useful discussions. This work has been supported in part by the Grants-in-Aid for Scientific Research (18540280) of Education, Science, Sports, and Culture of Japan.

-
- [1] J. Kogut, M. Stone, H. W. Wyld, W. R. Gibbs, J. Shigemitsu, S. H. Shenker, and D. K. Sinclair, Phys. Rev. Lett. **50**, 393 (1983).

model	T_e [MeV]	μ_e [MeV]	μ_e/T_e
NJL	0.047	0.330	7.0
NJL+ σ^4	0.062	0.276	4.5
NJL+ σ^4 ($M_\sigma = 650$ MeV)	0.054	0.308	5.7
NJL with vector interaction ($G_v = 0.25G_s$)	0.021	0.357	17
PNJL	0.111	0.325	2.9
PNJL+ σ^4	0.149	0.261	1.8
PNJL+ σ^4 ($T_0 = 170$ MeV)	0.118	0.250	2.1
PNJL with vector interaction ($G_v = 0.25G_s$)	0.052	0.357	6.9

TABLE III: The values of T_e , μ_e and μ_e/T_e in several models.

- [2] Z. Fodor and S. D. Katz, J. High Energy Phys. **03**, 014 (2002); Prog. Theor. Phys. Suppl. **153**, 86 (2004).
- [3] S. Ejiri, arXiv:hep-lat/0706.3549 (2007); arXiv:hep-lat/0710.0653 (2007).
- [4] Y. Nambu and G. Jona-Lasinio, Phys. Rev. **122**, 345 (1961); Phys. Rev. **124**, 246 (1961).
- [5] M. Asakawa and K. Yazaki, Nucl. Phys. **A504**, 668 (1989).
- [6] O. Scavenius, Á. Mócsy, I. N. Mishustin, and D. H. Rischke, Phys. Rev. C **64**, 045202 (2001).
- [7] O. Kiriya, M. Maruyama, and F. Takagi, Phys. Rev. D **63**, 116009 (2001).
- [8] Y. Hashimoto, Y. Tsue, and H. Fujii, Prog. Theor. Phys. **114**, 595 (2005).
- [9] R. A. Lacey, N. N. Ajitanand, J. M. Alexander, P. Chung, J. Jia, A. Taranenko, and P. Danielewicz, arXiv:nucl-ex/0708.3512 (2007).
- [10] K. Kashiwa, H. Kouno, T. Sakaguchi, M. Matsuzaki, and M. Yahiro, Phys. Lett. B **647**, 446 (2007).
- [11] D. Zschesche, G. Zeeb, S. Schramm and H. Stöcker, J. Phys. G: Nucl. Part. Phys. **31**, 935 (2005).
- [12] D. Zschesche, G. Zeeb, and S. Schramm, arXiv:nucl-th/0602073 (2006).
- [13] P. N. Meisinger, and M. C. Ogilvie, Phys. Lett. B **379**, 163 (1996).
- [14] K. Fukushima, Phys. Lett. B **591**, 277 (2004).
- [15] S. K. Ghosh, T. K. Mukherjee, M. G. Mustafa, and R. Ray, Phys. Rev. D **73**, 114007 (2006).
- [16] E. Megías, E. R. Arriola, and L. L. Salcedo, Phys. Rev. D **74**, 065005 (2006).
- [17] C. Ratti, M. A. Thaler, and W. Weise, Phys. Rev. D **73**, 014019 (2006).
- [18] C. Ratti, S. Rößner, M. A. Thaler, and W. Weise, Eur. Phys. J. C **49**, 213 (2007).
- [19] S. Rößner, C. Ratti, and W. Weise, Phys. Rev. D **75**, 034007 (2007).
- [20] H. Hansen, W. M. Alberico, A. Beraudo, A. Molinari, M. Nardi, and C. Ratti, Phys. Rev. D **75**, 065004 (2007).
- [21] C. Sasaki, B. Friman, and K. Redlich, Phys. Rev. D **75**, 074013 (2007).
- [22] B. -J. Schaefer, J. M. Pawłowski, and J. Wambach, Phys. Rev. D **76**, 074023 (2007).
- [23] M. Buballa, Nucl. Phys. **A611**, 393 (1996).
- [24] M. Kitazawa, T. Koide, T. Kunihiro, and Y. Nemoto, Prog. Theor. Phys. **108**, 929 (2002).
- [25] K. Kashiwa, M. Matsuzaki, H. Kouno, and M. Yahiro, Phys. Lett. B **657**, 143 (2007).
- [26] D. Blaschke, T. Klähn, and F. Sandin, arXiv:nucl-th/0708.4216 (2007).
- [27] A. A. Osipov, B. Hiller, and J. da Providência, Phys. Lett. B **634**, 48 (2006).

- [28] A. A. Osipov, B. Hiller, J. Moreira, and A. H. Blin, Eur. Phys. J. C **46**, 225 (2006).
- [29] A. A. Osipov, B. Hiller, J. Moreira, A. H. Blin, and J. da Providência, Phys. Lett. B **646**, 91 (2007).
- [30] A. A. Osipov, B. Hiller, J. Moreira, and A. H. Blin, arXiv:hep-ph/0709.3507 (2007).
- [31] J. I. Kapusta, *Finite-temperature field theory* (Cambridge University Press, 1989).
- [32] M. Le Bellac, *Thermal Field Theory* (Cambridge University Press, 1996).
- [33] G. Boyd, J. Engels, F. Karsch, E. Laermann, C. Legeland, M. Lütgemeier, and B. Petersson, Nucl. Phys. **B469**, 419 (1996).
- [34] O. Kaczmarek, F. Karsch, P. Petreczky, and F. Zantow, Phys. Lett. B **543**, 41 (2002).
- [35] T. Hatsuda, and T. Kunihiro, Prog. Theor. Phys. Phys. **74**, 765 (1985).
- [36] A. Barducci, R. Casalbuoni, G. Pettini, and R. Gatto, Phys. Lett. B **301**, 95 (1993).
- [37] F. Karsch, E. Laermann, and A. Peikert, Nucl. Phys. B **605**, 579 (2001).